Borozenes: Benzene-Like Planar Aromatic Boron Clusters

Lai-Sheng Wang*

Department of Chemistry, Brown University, Providence, RI 02912

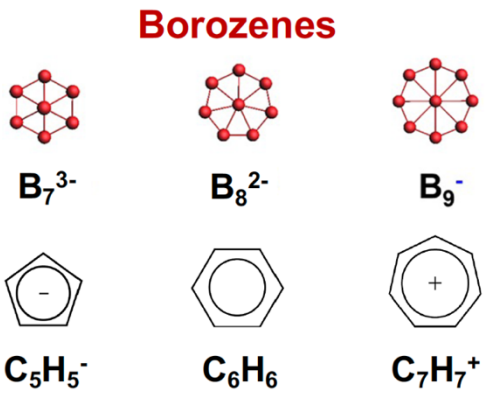

CONSPECTUS: With three valence electrons and four valence orbitals, boron ($2s^22p^1$) is an electron-deficient element, resulting in interesting chemical bonding and structures in both borane molecules and bulk boron materials. The electron deficiency leads to electron sharing and delocalization in borane compounds and bulk boron allotropes, characterized by polyhedral cages, in particular, the ubiquitous B_{12} icosahedral cage. During the past two decades, the structures and bonding of size-selected boron clusters have been elucidated via combined photoelectron spectroscopy and theoretical investigations. Unlike bulk boron materials, finite boron clusters have been found to possess 2D structures consisting of B_3 triangles, dotted with tetragonal, pentagonal, or hexagonal holes. The discovery of the planar B_{36} cluster with a central hexagonal hole provides the first experimental evidence for the viability of 2D boron nanostructures (borophene), which have been synthesized on inert substrates. The B_7^-, B_8^-, and B_9^- clusters were among the first few boron clusters to be investigated by joint photoelectron spectroscopy and theoretical calculations and they were all found to possess 2D structures with a central B atom inside a B_n ring. Recently, the B_7^{3-} (C_{6v}), B_8^{2-} (D_{7h}), and B_9^- (D_{8h}) series of closed-shell species are shown to possess similar π bonding akin to that in the $C_5H_5^-$, C_6H_6, and $C_7H_7^+$ series, respectively, and the name "borozene" is coined to highlight their analogy to the classical aromatic hydrocarbon molecules. Among the borozenes, the D_{7h} B_8^{2-} is unique for its high stability originating from both its double aromaticity and the fact that the B_7 ring has the perfect size to host a central B atom. The B_8^{2-} borozene has been realized experimentally in a variety of MB_8 and M_2B_8 complexes. In particular, the B_8^{2-} borozene has been observed to stabilize the rare valence-I oxidation state of lanthanides in LnB_8^- complexes, as well as a Cu_2^+ species in $Cu_2B_8^-$. The B_6 ring in B_7^{3-} is too small to host the B atom, resulting in a slight out-of-plane distortion. Interestingly, the bowl-shaped B_7 borozene is perfect to be coordinated to a metal atom, leading to the observation of a series of highly stable MB_7 borozene complexes. On the other hand, the B_8 ring is slightly too large to host the central B atom, such that a low-lying and low-symmetry isomer also exists for B_9^-. Even though most 2D boron clusters are aromatic, the B_7^{3-}, B_8^{2-} and B_9^- borozenes are special because of their high symmetries and their analogy to the series of $C_5H_5^-$, C_6H_6, and $C_7H_7^+$ prototypical aromatic compounds. This Account discusses recent experimental and theoretical advances on the investigations of various borozene complexes. It is expected that many new borozene compounds can be designed and may be eventually synthesized.

■ KEY REFERENCES

- Li, W. L.; Chen, T. T.; Chen, W. J.; Li, J.; Wang, L. S. Monovalent Lanthanide(I) in Borozene Complexes. *Nature Commun*. **2021**, *12*, 6467.[1] Photoelectron spectroscopy and computational study show that LnB_8^- clusters consist of a Ln(I) center interacting with a B_8^{2-} aromatic motif and the word "borozene" is first coined here to designate B_7^{3-}, B_8^{2-}, and B_9^-.
- Tian, W. J.; Chen, W. J.; Yan, M.; Li, R.; Wei, Z. H.; Chen, T. T.; Chen, Q.; Zhai, H. J.; Li, S. D.; Wang, L. S. Transition-Metal-Like Bonding Behaviors of a Boron Atom in a Boron Cluster Boronyl Complex $[(\eta^7\text{-}B_7)\text{-}B\text{-}BO]^-$. *Chem. Sci*. **2021**, *12*, 8157-8164.[2] The global minimum structure of the B_9O^- cluster is found to consist of a B atom sandwiched by a η^7-B_7 and a BO unit, revealing the stability of the B_7^{3-} borozene and a transition-metal-like central B atom.
- Chen, W. J.; Pozdeev, A. S.; Choi, H. W.; Boldyrev, A. I.; Yuan, D. F.; Popov, I. A.; Wang, L. S. Searching for Stable Copper Borozene Complexes in CuB_7^- and CuB_8^-. *Phys. Chem. Chem. Phys*. **2024**, *26*, 12928-12938.[3] The CuB_8^- cluster is found to be a stable B_8^{2-} borozene complex with C_{7v} symmetry, whereas the global minimum of CuB_7^- has an elongated double chain global minimum because it is one electron short of a B_7^{3-} borozene complex.
- Chen, W. J.; Choi, H. W.; Cavanagh, J.; Yuan, D. F.; Wang, L. S. Electronic Control of the Position of the Pb Atom on the Surface of the B_8 Borozene in the PbB_8 Cluster. *J. Phys. Chem. A* **2024**, *128*, 3564-3570.[4] Neutral PbB_8 is found to be a highly stable C_{7v} $Pb^{2+}[B_8^{2-}]$ borozene complex, whereas the Pb atom is significantly distorted from the C_7 axis in the PbB_8^- anion due to strong Jahn-Teller effect.

1. INTRODUCTION

As neighbors in the periodic table, boron and carbon share some similarities. They both have multiple allotropes with high melting temperatures and can form strong covalent bonds through catenation. By acquiring an extra electron, boron behaves just like carbon, as revealed in the graphene-like boron layer in MgB_2 or the carbyne-like boron chains in LiB solid compounds.[5,6] However, the apparent electron deficiency of boron results in much more complicated chemical bonding and structures in both boron-containing molecules and bulk boron allotropes. Boron is known as the "rule breaker" because most of the chemical rules are based on carbon chemistry and the octet rule. The electron deficiency of boron leads to multicenter bonding and electron delocalization in boranes and all known boron allotropes, characterized by polyhedral cages, in particular, the B_{12} icosahedral cage.[7,8] The investigation of carbon clusters toward the end of the twentieth century led to the discovery of a rich variety of nanostructures from the fullerenes to carbon nanotubes and graphenes.[9-11] To examine the possibility of similar nanostructures for other elements, our lab and collaborators have embarked on a comprehensive investigation of size-selected boron clusters at the beginning of the twenty first century using anion photoelectron

spectroscopy (PES) and computational chemistry.[12-17] We have found that small boron clusters all have planar (2D) structures, in stark contrast to the 3D polyhedral cages that are the building blocks of bulk boron. Apparently, electron delocalization in 2D planes both in the σ and π frameworks is more energetically favorable in finite boron clusters, leading to σ and π double aromaticity. The π bonding patterns in most planar boron clusters can be compared with that in polycyclic aromatic hydrocarbons, leading to the concept of boron clusters as hydrocarbon analogs.[18-20] The discovery of the planar B_{36} cluster with a central hexagonal vacancy provided the first experimental evidence for the viability of stable 2D boron with a triangular lattice dotted with hexagonal holes. A name "borophene" was coined to designate the novel 2D boron,[21] which has been synthesized on inert substrates[22,23] and is becoming a new class of synthetic 2D nanomaterials.[24] The B_{40} cluster was found to have a cage structure, the first all-boron fullerene (borospherene).[25]

The first boron cluster that was investigated by joint PES and theoretical study was B_5^-,[26] followed by B_6^-,[27] B_8^- and B_9^-,[28] and B_n^- (n = 10–15).[18] The global minimum of B_9^- was found to have a beautiful D_{8h} closed-shell structure with a central B atom inside a B_8 ring. The B_8 ring was shown to be bonded by eight 2-center 2-electron (2c-2e) bonds, whereas the bonding between the central B atom and the B_8 ring was via three delocalized 9c-2e σ bonds and three delocalized 9c-2e π bonds, giving rise to double aromaticity for B_9^-. Despite the fact that the neutral B_8 cluster has an even number of electrons, the PES of B_8^- did not reveal a HOMO-LUMO gap, because the neutral B_8 cluster was found to have a high symmetry open-shell D_{7h} structure with two unpaired electrons in a doubly degenerate orbital ($1e_1''$).[28] The B_8^- anion was found to have a planar C_{2v} structure due to the Jahn-Teller effect, whereas the B_8^{2-} species (D_{7h}) was shown to be closed shell with a bonding situation similar to that in B_9^- and it was subsequently observed in the form of LiB_8^- ($Li^+[B_8^{2-}]$).[29] The PES of B_7^- was observed to be quite complicated and it took more than two years to be solved.[30] It turned out that there were two low-lying isomers present and the global minimum of B_7^- was open-shell with a C_{6v} ($^3A_1$) structure. In a recent study on lanthanide-doped octaboron clusters (LnB_8^-),[1] it was recognized that the closed-shell molecular wheels, B_7^{3-}, B_8^{2-}, and B_9^- all have similar structures and bonding, and their π bonds are all similar to benzene, as shown in Figure 1. In fact, the trends of charge and molecular size from B_7^{3-} to B_8^{2-} to B_9^- are analogous to the cyclic aromatic $C_5H_5^-$, C_6H_6, $C_7H_7^+$, respectively. A name "borozene" was coined for the three closed-shell and highly symmetric boron clusters to underline their similarity with the classical aromatic hydrocarbons.

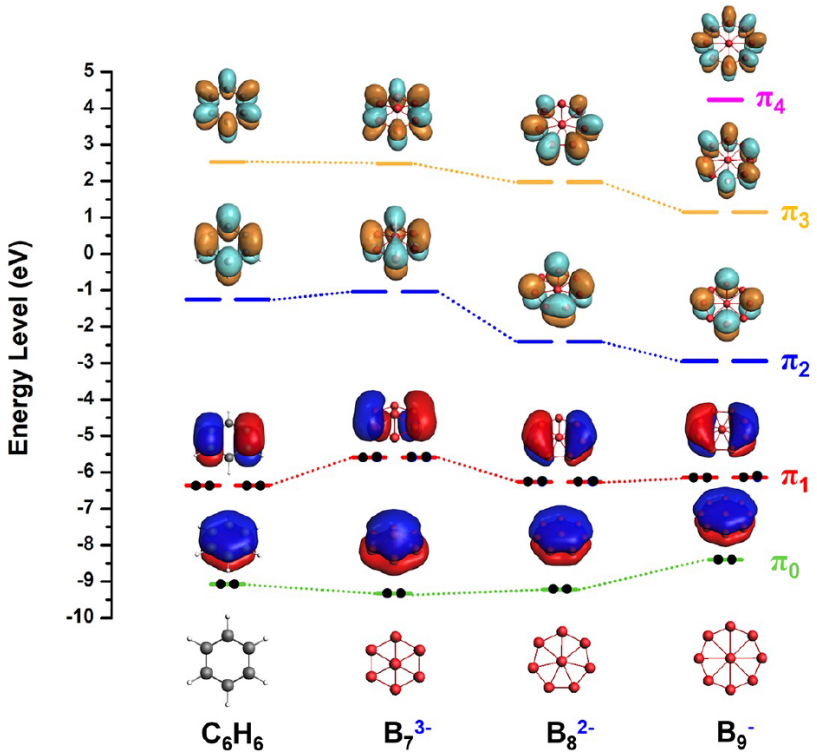

Figure 1. Comparison of the π orbitals of borozenes, B_7^{3-}, B_8^{2-}, and B_9^- with those of benzene. Only one molecular orbital is shown for the degenerate π orbitals. The dots denote the π electrons. Adapted with permission from ref. 1. Copyright 2021 Springer Nature Limited.

While transition metal doping may change the structures of the planar boron clusters,[16,31-33] dopants with low electronegativity or the right electronic properties can form borozene complexes. A number of borozene complexes have been observed experimentally and studied computationally. This Account will discuss these advances and in particular the recent experimental observations of B_7^{3-} and B_8^{2-} borozene complexes. The B_7 ring is perfect in size in the B_8^{2-} borozene, resulting in highly stable borozene complexes, such as the stabilization of the rare Ln(I) oxidation state in the LnB_8^- complexes.[1] The B_6 ring in the B_7^{3-} borozene is too small, squeezing the central B atom slightly out of plane. The bowl-shaped B_7 borozene is conducive to η^7-coordination to another atom, resulting in the surprising umbrella structure in B_9O^- (η^7-B_7-B-BO^-).[2] The B_8 ring in the B_9^- borozene is slightly too large to host the central B atom, leading to a low-lying isomer for B_9^-.[34] No MB_9^- type borozene complexes have been observed experimentally, which would require a valence zero M atom. However, neutral MB_9 complexes should be viable for valence-I atoms, such as the alkali elements.[35]

2. B_7^{3-} BOROZENE COMPLEXES

2.1. MB_7 Borozene Complexes for M = Valence III Elements

2.1.1. AlB_7^- and AlB_7. The C_{6v} global minimum of B_7^- has a triplet ($^3A_1$) ground state with two unpaired electrons in a doubly degenerate HOMO ($3e_1$).[30] Filling the $3e_1$ HOMO with two more electrons would yield the closed-shell B_7^{3-} borozene (Figure 1). Thus, valence III elements are expected to form highly stable MB_7 borozene complexes. The first B_7^{3-} borozene complex observed was AlB_7^-, which was investigated by PES and theoretical calculations.[36] It was found to have a C_{6v} structure with a doublet ($^2A_1$) spin state, where the unpaired electron occupied an MO mainly of Al 3*s* character. However, neutral AlB_7 was found to have a C_{2v} structure with a triplet electronic state ($^3B_1$), because the first electron detachment occurred from the degenerate $3e_1$ MO on the B_7 motif. Consequently, the AlB_7 cluster did not form the expected $Al^{3+}[B_7^{3-}]$ borozene complex. Instead, it should be viewed as $Al^{2+}[B_7^{2-}]$; apparently it is energetically unfavorable to transfer the second 3*s* electron of Al to the B_7 motif. Interestingly, a recent study on CuB_7^- shows that, though its global minimum involves a double chain B_7 motif with a terminal Cu atom, the borozene complex (C_{2v} $Cu^+[B_7^{2-}]$) is very close in energy, which was observed experimentally to coexist with the global minimum.[3] The B_7^{2-} borozene in both cases is open-shell with five delocalized π electrons and there is a Jahn-Teller distortion to C_{2v} symmetry.

2.1.2. PrB_7^- and PrB_7. The favorite oxidation state of lanthanides is +III, which gives rise to the first B_7^{3-} borozene complex in PrB_7.[37] The PES of PrB_7^- revealed a large HOMO-LUMO gap (the X–A gap in Figure 2), suggesting a highly stable neutral PrB_7. Theoretical calculations showed that PrB_7^- has a perfect C_{6v} structure with three unpaired electrons (one in the Pr 6*s* orbital and two

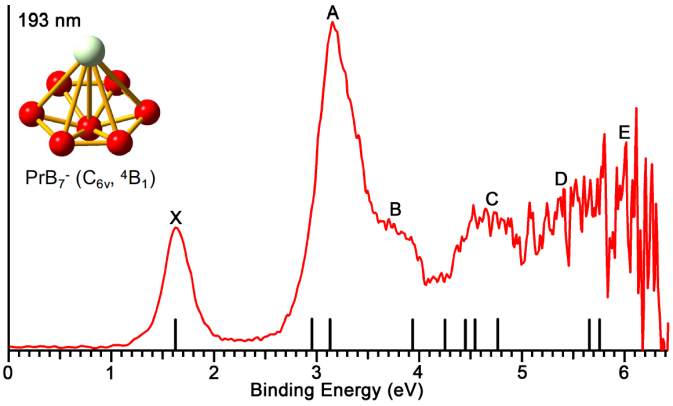

Figure 2. The photoelectron spectrum of PrB_7^- at 193 nm. The inset shows the structure and symmetry of PrB_7^-. The vertical bars indicate the computed detachment channels from the C_{6v} PrB_7^-. Adapted with permission from ref. 37. Copyright 2017 Wiley-VCH.

in the localized Pr 4*f* orbitals). Detachment of the 6*s* electron results in the perfect PrB_7 borozene complex ($Pr^{3+}[B_7^{3-}]$), as borne out by the AdNDP chemical bonding analysis (Figure 3).[38] The AdNDP results revealed the six 2c-2e bonds on the peripheral B_6 ring of the B_7 motif, the three delocalized σ bonds and the three delocalized π bonds on the B_7^{3-} borozene. The π bonds embody *d*-π interactions between Pr and B_7. A previous computational study indicated that the isovalent ScB_7 cluster has a closed-shell C_{6v} structure, which was shown to be highly stable with a large HOMO-LUMO gap.[39] All rare-earth and lanthanide elements should form stable borozene complexes of the $M^{3+}[B_7^{3-}]$ type.

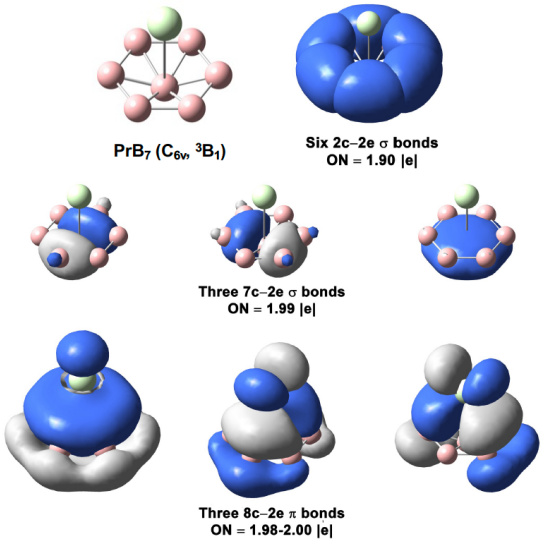

Figure 3. The AdNDP bonding analysis for PrB_7. The two localized 4*f* electrons on Pr are not shown. Note the three bonding components on the B_7^{3-} borozene: 1) the six 2c-2e σ bonds on the peripheral B_6 ring, 2) the three 7c-2e delocalized σ bonds, and 3) the three 8c-2e delocalized π bonds involving *d*-π interactions between Pr and the borozene. The structure and symmetry of neutral PrB_7 are shown on the top (left). ON indicates the occupation number. Adapted with permission from ref. 37. Copyright 2017 Wiley-VCH.

2.1.3. The BiB_7 Borozene Complex, and Ionic and *p*-π Covalent Bonding between the Dopant and the B_7 Borozene. The BiB_7^- cluster has been studied recently by PES and theoretical calculations.[40] The global minimum of BiB_7^- was found to be planar with the Bi atom bonded to the side of a B_7 motif, which can be viewed as substituting one peripheral B atom in B_8^- by a Bi atom. However, the C_{6v} borozene complex is overwhelmingly the global minimum for neutral BiB_7, in which Bi has an oxidation state of +III with a 6*s* lone pair. The AdNDP bonding analysis for BiB_7 is given in Figure 4, which clearly reveals the 6*s* lone pair on Bi, the six 2c-2e σ bonds on the B_6 ring of B_7, the three delocalized σ bonds, and the three delocalized π bonds. The Bi 6*p* orbitals engage in *p*-π interactions with the borozene, giving rise to an extremely stable BiB_7

complex. A previous computational study suggested that the isovalent PB_7 cluster also has a similar C_{6v} structure.[41] A recent computational study on GeB_7 also showed a C_{7v} global minimum structure.[42]

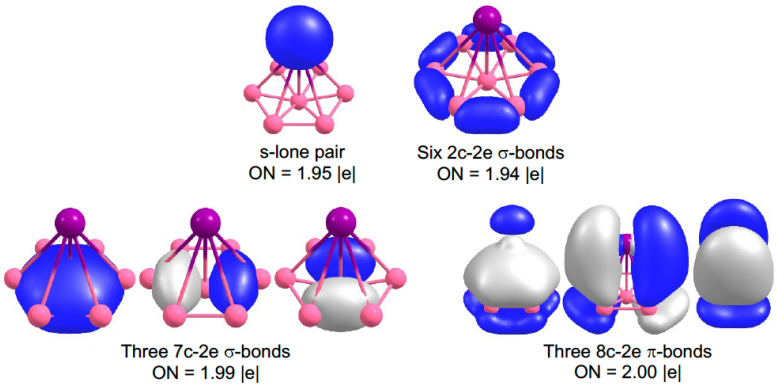

Figure 4. The AdNDP bonding analysis for BiB_7. Note the 6*s* lone pair on Bi and the three characteristic bonding components on the borozene: 1) the six 2c-2e σ bonds on the peripheral B_6 ring, 2) the three 7c-2e delocalized σ bonds, and 3) the three 8c-2e delocalized π bonds involving *p*-*π* interactions between Bi and the borozene. Adapted with permission from ref. 40. Copyright 2021 American Chemical Society.

The group IIA element Mg has been shown computationally to form a stable MgB_7^- borozene complex, $Mg^{2+}[B_7^{3-}]$.[43] It is safe to say that all valence II elements, both IIA and IIB, are expected to form stable MB_7^- type borozene complexes. Interestingly, $M_2B_7^-$ type clusters with group IIA and IIB elements have also been predicted computationally to form borozene complexes involving an M_2^{2+} dimer bond, $[M_2^{2+}][B_7^{3-}]$.[44,45] The group IIA and IIB elements are closed shell and their dimers cannot form stable covalent bonds. However, ligan-protected L-M(I)-M(I)-L type compounds have been synthesized with a single M(I)-M(I) σ bond for group IIA and IIB elements.[46-48] It is remarkable that the B_7^{3-} borozene can stabilize the M(I)-M(I) bonds in $[M_2^{2+}][B_7^{3-}]$ primarily through ionic interactions. In fact, binary $Na_6B_7^-$ and $Na_8B_7^+$ clusters have even been predicted to contain the B_7^{3-} borozene sandwiched by two Na clusters, i.e., $[Na_3^+][B_7^{3-}][Na_3^+]$ and $[Na_4^{2+}][B_7^{3-}][Na_4^{2+}]$, respectively.[49] Apparently, the high charge state of the B_7^{3-} borozene provides tremendous flexibility to design novel borozene complexes.

2.2. B_9O^-: A Surprising B_7 Borozene Complex, $[\eta^7\text{-}B_7\text{-}B\text{-}BO]^-$

The B_7 borozene complexes do not always require a charge transfer to form the B_7^{3-} species, such as in the alkali-B_7 complexes, where ionic interactions dominate. The B_7^{3-} borozene electronic structure in MB_7 complexes can also be fulfilled through covalent interactions between M and B_7, as seen above for BiB_7. There is strong covalent interaction in the BiB_7 borozene complex between

the 6*p* orbitals of Bi and the π orbitals on B_7 (Figure 4), because the electronegativities of B and Bi are similar. The most surprising B_7 borozene complex was observed in the B_9O^- cluster, which contains a MB_7 motif with M = B (**1** in Figure 5).

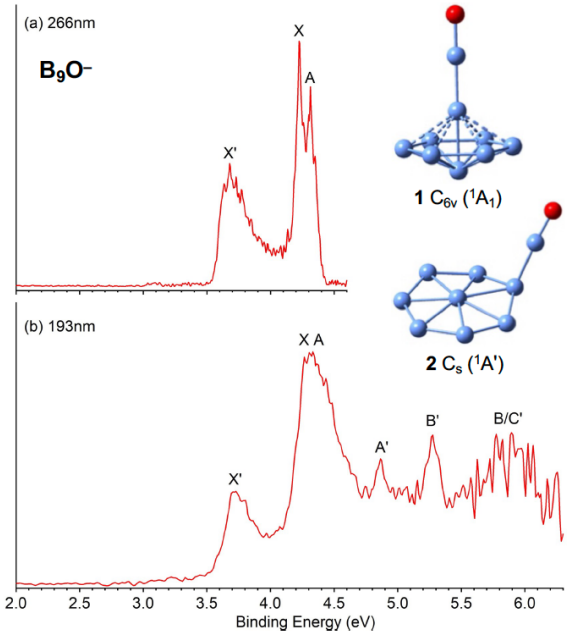

Figure 5. The photoelectron spectra of B_9O^- at (a) 266 nm and (b) 193 nm. The inset shows the two isomers of B_9O^- responsible for the observed spectra. The observed spectral features, X, A, B, come from the global minimum isomer **1**; the features, X', A', B', C', come from the close-lying isomer **2**. Adapted with permission from ref. 2. Copyright 2021 Royal Society of Chemistry.

The photoelectron spectra of B_9O^- (Figure 5) were fairly complicated for a closed shell species. Temperature-dependent PES revealed that the observed photoelectron spectra contained contributions from two isomers. Structure searches led to two close-lying isomers (inset in Figure 5). Structure **2** consisting of a planar B_8 motif bonded to a BO unit on the periphery was expected, but it was not the global minimum. The umbrella-shaped structure **1** turned out to be the global minimum, which was a complete surprise. Structure **1** consists of a central B atom sandwiched by a B_7 motif and a BO unit. The more intense spectral features (X, A, B) in Figure 5 came from the global minimum structure **1**. The AdNDP analysis (Figure 6) clearly revealed the B_7 borozene bonding motif for structure **1**, through covalent bonding existed between the *p* orbitals on the central B atom and the π orbitals on the B_7 motif. The central B atom is coordinated by the B≡O boronyl unit on the other side.

Not only was the umbrella structure for B_9O^- a surprise, the bonding modes of the central B atom were also highly unusual. The half-sandwich coordination by borozene to the central B atom

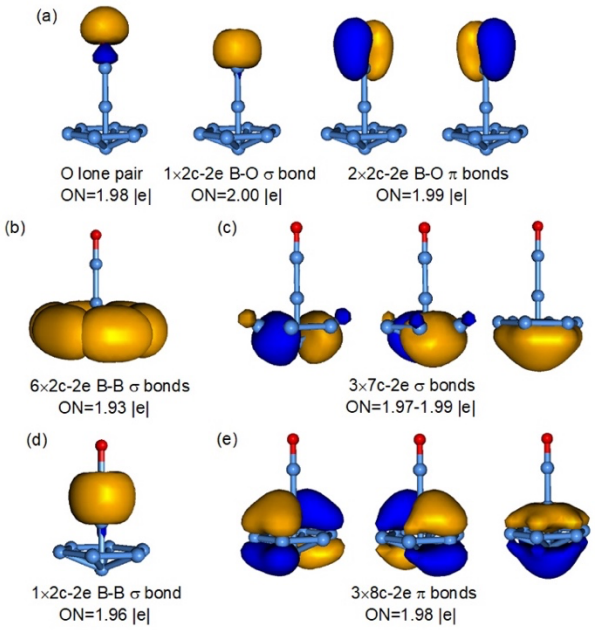

Figure 6. The AdNDP bonding analysis for the global minimum umbrella structure **1** of B_9O^-. Note the bonding features for the borozene: the six 2c-2e σ bonds (b), the three 7c-2e delocalized σ bonds (c), and the three 8c-2e delocalized π bonds (e). The BO unit (a) is bonded to the central B atom via a 2c-2e σ bond (d). Adapted with permission from ref. 2. Copyright 2021 Royal Society of Chemistry.

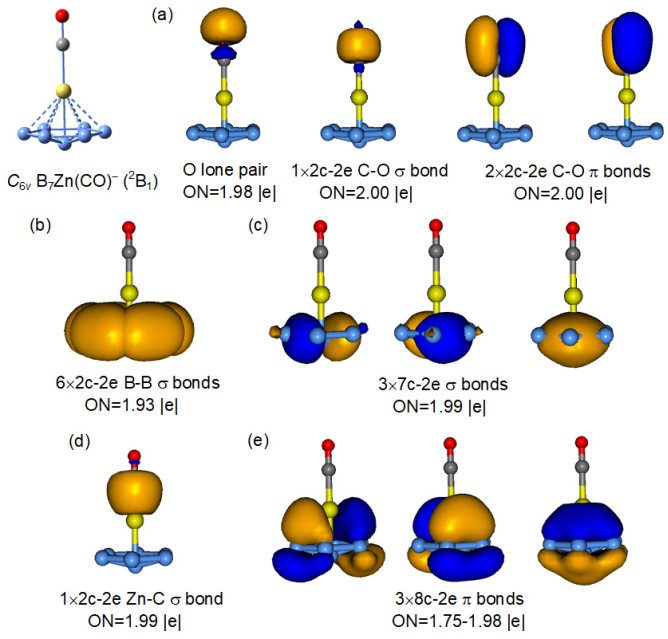

Figure 7. The AdNDP bonding analysis for the η^7-B_7-Zn-CO^- complex for comparison with that of B_9O^- in Figure 6. Adapted with permission from ref. 2. Copyright 2021 Royal Society of Chemistry.

is reminiscent of coordination by arenes to a transition metal center. Since the BO^- unit is isoelectronic to CO,[50] the BO coordination to the central B atom also imitates the bonding mode

between a transition metal with a CO ligand. Thus, the central B atom in the umbrella structure really behaves like a transition metal. To illustrate the metallomimetic properties of the central B atom, Figure 7 displays the chemical bonding of a model Zn-borozene and CO complex, [η^7-B_7-Zn-CO^-]. Since the 3*d* electrons of Zn do not participate in bonding, the Zn complex can be considered to be isoelectronic to the umbrella B_9O^-. Their bonding is nearly identical (Figures 6 and 7). The bonding in [η^7-B_7-Fe$(CO)_3^-$] was also analyzed to compare with that of the C_{6v} B_9O^-.[2] It was found that the bonding between the B_7 borozene and Fe is similar to that between the B_7 borozene and the central B atom in [η^7-B_7-B-BO^-]. Thus, the central B atom has two of the most important bonding properties of a transition metal, i.e., the ability to form carbonyl complexes and sandwich complexes with arenes. The metallomimetic chemistry of boron has been well recognized in boron chemistry and has been harnessed to synthesize novel boron compounds.[51]

3. B_8^{2-} BOROZENE COMPLEXES

3.1. LnB_8^-: Stabilization of the Rare Ln(I) Oxidation State

The lack of a HOMO-LUMO gap in the photoelectron spectra of B_8^- was confirmed by theoretical calculations that revealed a highly symmetric disk-like neutral B_8 (D_{7h}) with a half-filled $1e_1$" HOMO.[28] Thus, adding two electrons to B_8 resulted in the closed-shell and highly stable D_{7h} B_8^{2-} (Figure 1), which is doubly aromatic with six delocalized σ and six delocalized π electrons. The B_8^{2-} species was first observed in LiB_8^-, whose photoelectron spectrum was much simpler and bore similarities to that of B_8^-.[29] The first B_8^{2-} complex was observed in AlB_8^-, which can be viewed as an $Al^+[B_8^{2-}]$ complex with a 3*s* lone pair on Al.[36] In fact, the AlB_8 neutral also has C_{7v} symmetry with a single 3*s* electron on Al, i.e., an $Al^{2+}[B_8^{2-}]$ complex.

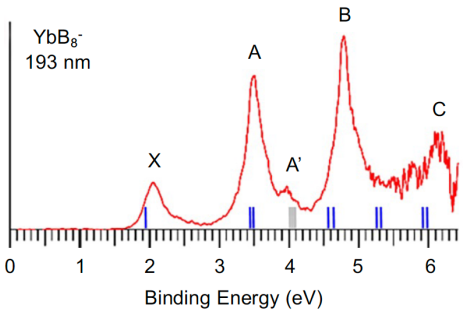

Figure 8. The 193 nm photoelectron spectrum of YbB_8^-. The vertical lines represent the computed vertical detachment energies. The gray bar denotes detachment from the 4*f*-based MOs, which have weak detachment cross sections. Adapted with permission from ref. 1. Copyright 2021 Springer Nature Limited.

A remarkable series of B_8^{2-} borozene complexes were discovered for the lanthanide elements (LnB_8^-) more recently, through a joint PES and theoretical investigation.[1] Photoelectron spectra of all the LnB_8^- clusters displayed similar PES features, though YbB_8^- gave the simplest spectrum (Figure 8), because Yb has a filled 4*f* shell. Global minimum searches showed that all the LnB_8^- clusters have C_{7v} structures (Figure 9), except for the early lanthanides for which a 3D isomer featuring a more distorted B_8 motif was found to be slightly lower in energy. The planar B_8^{2-} borozene motif was slightly distorted to a bowl shape upon complexation to the Ln atom.

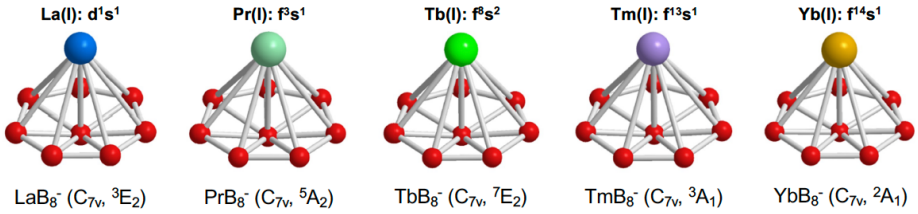

Figure 9. The C_{7v} structures for the LnB_8^- clusters, their symmetries, and the Ln(I) electron configurations. Note that for the early lanthanides (La and Pr) a 3D structure is slightly more stable in energy. Adapted with permission from ref. 1. Copyright 2021 Springer Nature Limited.

Chemical bonding analyses revealed that all the LnB_8^- complexes can be viewed as a B_8^{2-} borozene complexed to a Ln(I) center, in other words, the Ln atoms are in their +I oxidation state in the $Ln^+[B_8^{2-}]$ complexes. Figure 10 shows the AdNDP bonding analysis for YbB_8^-. In addition to the filled 4*f* shell and the localized 6*s* electron, one can clearly see the three characteristic bonding components of the B_8^{2-} borozene: the seven 2c-2e σ bonds on the B_7 ring, the three delocalized 8c-2e σ bonds, and the three delocalized 9c-2e π bonds. All the LnB_8^- complexes show similar bonding properties, except that the early lanthanides have unpaired 4*f* electrons, which do not participate in chemical bonding with the borozene. There is relatively weak *d*-π interaction between Ln and the borozene, indicating that there is strong charge transfer from Ln to B_8 and that ionic interactions are dominant in the LnB_8^- complexes. Even though the favorite oxidation state of the lanthanide elements is +III, the B_8^{2-} borozene has the unique capacity to stabilize the rare +I oxidation state for the lanthanides. It was during this study that the analogies in bonding and trends in charge state and molecular size between B_7^{3-}, B_8^{2-} and B_9^- and the cyclic aromatic $C_5H_5^-$, C_6H_6, and $C_7H_7^+$, respectively, were recognized, leading to the coining of the word "borozene" for the three benzene-like aromatic boron clusters.[1] Very recently, a computational study has shown that the actinide (An) elements form similar AnB_8^- borozene complexes, in which the B_8^{2-} borozene is able to stabilize the rare An(I) oxidation state.[52]

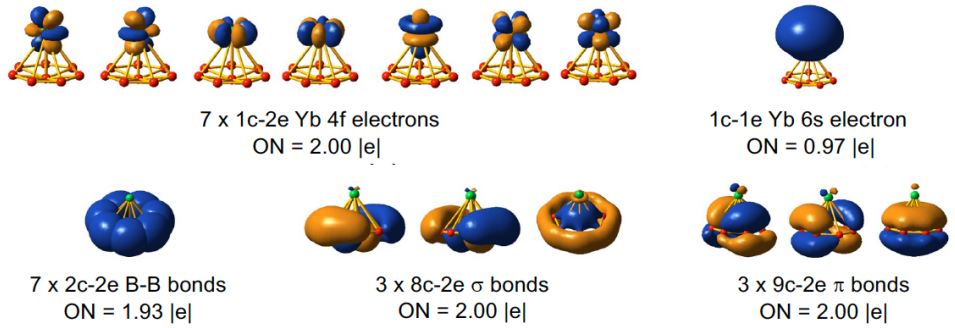

Figure 10. The AdNDP analysis for the C_{7v} YbB_8^- cluster. Note the localized 4*f* and 6*s* electrons on the Yb center and the three characteristic bonding component of the B_8^{2-} borozene: 1) the seven 2c-2e σ bonds on the B_7 ring, 2) the three delocalized σ bonds, and 3) the three delocalized π bonds. Adapted with permission from ref. 1. Copyright 2021 Springer Nature Limited.

3.2. CuB_8^- and $Cu_2B_8^-$ Borozene Complexes

Copper is an important substrate for the growth of borophenes. Copper-boron binary clusters are ideal systems to study the interactions between copper and boron, which may provide insight into the underlying growth mechanisms of borophenes on copper substrates. Significant charge transfers have been observed between the copper substrate and the borophene layer, which was suggested to be critical for the growth of bilayer borophenes on copper substrates.[53] In small Cu-B binary clusters, both covalent and ionic interactions have been observed between copper and boron.[54,55] The CuB_8^- cluster gave rise to a very simple photoelectron spectrum (Figure 11),[3] suggesting that it must have a high symmetry structure. Global minimum searches showed that it is a closed-shell C_{7v} cluster with the planar B_8 motif coordinated to the Cu atom (inset of Figure 11). Comparison between the computed vertical detachment energies and the experimental data

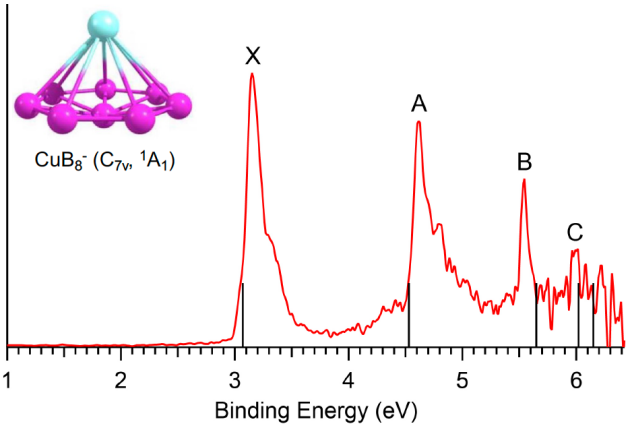

Figure 11. The photoelectron spectrum of CuB_8^- at 193 nm, compared with the computed vertical detachment energies of the global minimum C_{7v} structure (vertical lines). Adapted with permission from ref. 3. Copyright 2024 PCCP Owner Societies.

confirmed the C_{7v} structure. The AdNDP bonding analysis (Figure 12a) shows that CuB_8^- is basically a charge transfer complex between Cu^+ and the B_8^{2-} borozene. However, because of the strong relativistic stabilization of the 6*s* electron in gold,[56] Au tends to form covalent bonds[57] and the isovalent AuB_8^- cluster does not form a charge transfer complex. Instead, the Au atom is covalently bonded to the edge of the planar B_8 cluster.[58]

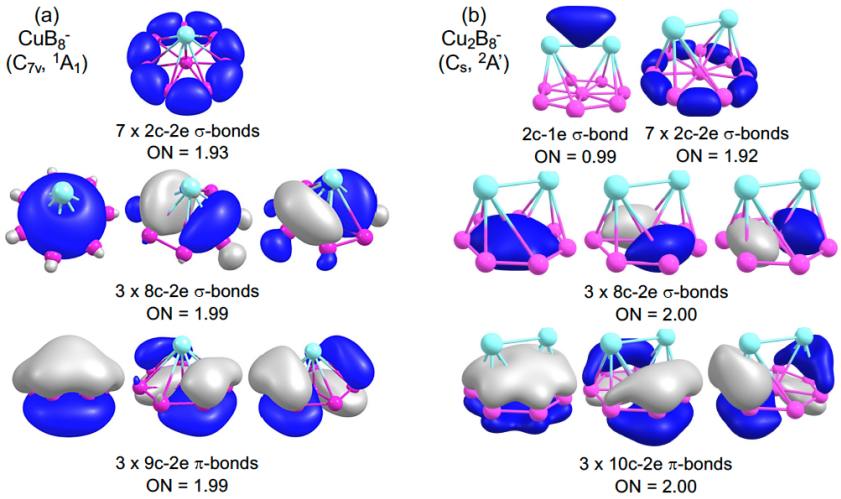

Figure 12. The AdNDP bonding analyses for (a) CuB_8^- and (b) $Cu_2B_8^-$. Both can be viewed as charge transfer complexes containing the B_8^{2-} borozene. (a) adapted with permission from ref. 3. Copyright 2024 PCCP Owner Societies. (b) adapted with permission from ref. 59. Copyright 2022 American Institute of Physics.

The di-cupper $Cu_2B_8^-$ cluster has also been studied by PES in conjunction with theoretical calculations.[59] Its global minimum was found to consist of a Cu_2 dimer above the planar B_8 cluster. The $Cu_2B_8^-$ cluster can be viewed as a charge transfer complex between the B_8^{2-} borozene and a Cu_2^+ unit with a single electron Cu−Cu bond, as revealed by the AdNDP bonding analysis (Figure 12b). The bonding in both $Cu^+[B_8^{2-}]$ and $[Cu_2^+][B_8^{2-}]$ is primarily ionic. A double chain B_8 motif with terminal Cu−B covalent bonding was found to be a higher energy isomer for both CuB_8^- and $Cu_2B_8^-$. It is remarkable that the B_8^{2-} borozene is able to stabilize a weakly bonded Cu_2^+ dimer. Neutral Cu_2B_8 has no Cu−Cu bonding and it can be viewed as two Cu^+ ions interacting ionically with the borozene, $(Cu^+)_2[B_8^{2-}]$.[59]

A previous computational study showed that Mg and Mg_2 both form B_8^{2-} borozene complexes in MgB_8^- and $Mg_2B_8^-$,[43] which can be viewed as $Mg^+[B_8^{2-}]$ and $[Mg_2^+][B_8^{2-}]$, respectively. Another theoretical study suggests that the neutral Mg_2B_8 cluster consists of a "nanoscale compass",[60] where the singly-bonded $[Mg_2]^{2+}$ dimer can almost freely rotate relative to the B_8^{2-} borozene with a very low rotation barrier due to the nature of the ionic interactions. Similar to the

B_7^{3-} borozene in $Mg_2B_7^-$, the B_8^{2-} borozene is also able to stabilize a Mg(I)-Mg(I) σ bond through ionic interactions in Mg_2B_8. It is expected that all M_2B_8 clusters for groups IIA and IIB elements should form similar borozene complexes with a M(I)-M(I) σ bond,[44] and all MB_8 clusters should form $M^{2+}[B_8^{2-}]$ type closed-shell borozene complexes.

3.3. Electronic Control of the Pb Atom Position on the B_8 Borozene Surface

Due to the strong relativistic effects,[56] the 6*s* electrons of the Pb atom are chemically inert and Pb(II) is a common oxidation state. Thus, the PbB_8 cluster is expected to be a highly stable $Pb^{2+}[B_8^{2-}]$ borozene complex, similar to the borozene complexes with group IIA or IIB elements. Indeed the photoelectron spectrum of PbB_8^- showed a large HOMO-LUMO gap (defined by the separation between peaks X and A in Figure 13), evident of the high electronic stability of neutral PbB_8.[4] Furthermore, the ground state detachment transition (band X) was very broad, indicating a

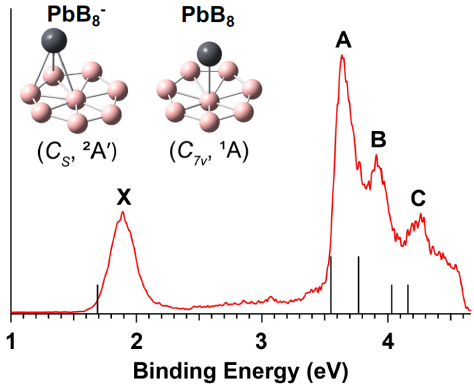

Figure 13. The photoelectron spectrum of PbB_8^- at 266 nm. The inset shows the global minimum structures of PbB_8^- (C_s) and neutral PbB_8 (C_{7v}). The vertical lines represent the computed vertical detachment energies from the C_s PbB_8^-. The shorter lines indicate singlet final states and the longer lines indicate triplet final states. Adapted with permission from ref. 4. Copyright 2024 American Chemical Society.

large geometry change between the PbB_8^- anion and the PbB_8 neutral. Computational studies found that indeed the neutral PbB_8 has a highly symmetric and stable C_{7v} structure, while the PbB_8^- anion has a C_s symmetry with the Pb atom moving significantly away from the C_7 axis (see inset in Figure 13). The large geometry change between the anion and neutral is consistent with the broad PES band X of PbB_8^- and was confirmed by Franck-Condon factor calculations.[4] In fact, the PbB_8^- anion is isoelectronic to BiB_8, and both have similar C_s structures.[40]

Results from the AdNPD bonding analysis for PbB_8 revealed a clear $Pb^{2+}[B_8^{2-}]$ borozene complex (Figure 14). In addition to the 6*s* lone pair, the three bonding characteristics of the B_8^{2-} borozene can be seen readily: the seven 2c-2e σ bonds on the B_7 ring and the three delocalized σ

and π bonds. The three π bonds exhibit significant *p*-π bonding interactions between Pb and the borozene, similar to the *p*-π bonding in the BiB_7 borozene complex (Figure 4).

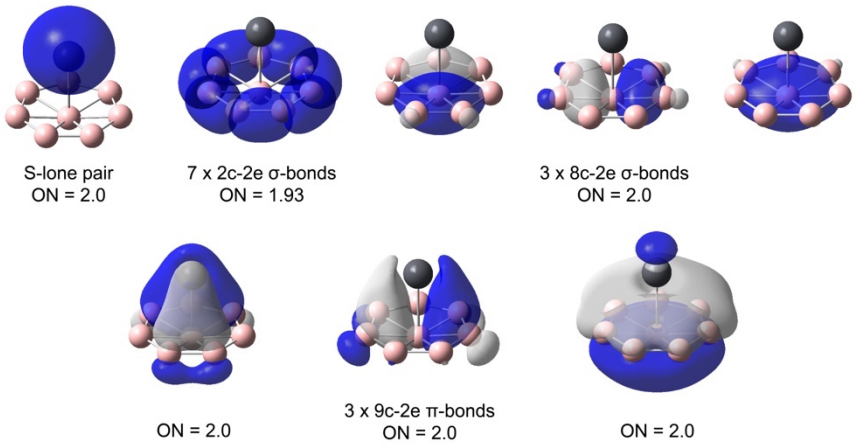

Figure 14. The AdNDP bonding analyses for PbB_8. Adapted with permission from ref. 4. Copyright 2024 American Chemical Society.

The LUMO of PbB_8 consists of a degenerate orbital (e_1). Occupation of the e_1 LUMO in the PbB_8^- anion induces a Jahn-Teller distortion that lowers the symmetry of the anion. However, what is surprising is the large amplitude of the Pb distortion. It turns out that the LUMO represents anti-bonding *p*-π interactions between Pb and B_8. The large shift of the Pb atom from the C_7 axis essentially reduces the anti-bonding interactions, maintaining the integrity of the B_8^{2-} borozene. PbB_8^- can be viewed as a $Pb^+[B_8^{2-}]$ complex with a Pb(I) center. Thus, the position of the Pb atom on the surface of the B_8^{2-} borozene is controlled by the addition or removal of an electron, which can be viewed as a new type of molecular switch (Figure 15).

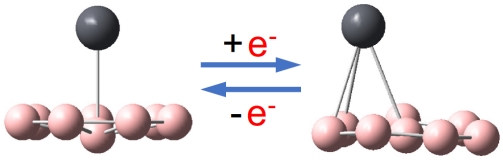

Figure 15. A schematic for an electron switch, showing the change of the position of the Pb atom on the surface of the B_8 borozene upon the addition or removal of an electron.

Ionic interactions are important to stabilize the B_8^{2-} borozene, as shown by the LnB_8^- and CuB_8^- or $Cu_2B_8^-$ complexes above. As shown in Figure 14, *p*-π bonding interactions can also be involved in forming MB_8 borozene complexes. A previous calculation showed a C_{7v} PB_8^+ cluster,[61] which can be considered to be a *p*-π B_8 borozene complex, where the P^+ center shares its two 3*p* electrons with the B_8^{2-} borozene. Similar *p*-π borozene complexes have also been found computationally

for C_{7v} SiB_8 and GeB_8.[41,42,62] Carbon forms strong C–B covalent bonds and C is known to be incorporated in the peripheral position of the planar CB_8 cluster,[63] which is in fact isoelectronic to the B_9^- borozene. Apparently, the heavier group IVA elements from Si to Pb with more radially extended valence *p* orbitals favor the formation of C_{7v} type MB_8 borozene complexes. Similarly, the heavier group VA cations from P^+ to Bi^+ can form C_{7v} type MB_8^+ borozene complexes. All these C_{7v} MB_8 or MB_8^+ borozene complexes should exhibit similar electron switching properties as illustrated in Figure 15, forming a new class of molecular switches.

4. SUMMARY AND OUTLOOK

This Account focuses on the concept of borozenes, a class of planar boron clusters (B_7^{3-}, B_8^{2-}, and B_9^-) with delocalized π bonding akin to classical cyclic aromatic hydrocarbon molecules, as well as recent advances on the experimental observation and characterization of borozene complexes, in particular complexes of the B_7^{3-} and B_8^{2-} borozenes with elements of low electronegativity. Valence-III elements can form highly stable borozene complexes with B_7^{3-} (MB_7), while valence-II elements can form stable complexes with the B_8^{2-} borozene (MB_8). The high charge states of B_7^{3-} and B_8^{2-} provide significant flexibility to design novel borozene complexes. In addition to charge transfer complexes, *d*-π and *p*-π bonding interactions between the dopant and the borozenes are also important to form borozene complexes. While the current Account focuses on the recent advances in the investigation of complexes formed by the B_7^{3-} and B_8^{2-} borozenes, the potential of this field and the implication of the insight obtained thus far are huge. In addition to other novel B_7- or B_8-borozene complexes, there has been little study on the B_9^- borozene complexes heretofore. The prospect to use borozene complexes as a new platform for molecular switches is also intriguing. Going beyond borozenes, there are also enormous potentials to form other novel doped boron clusters. The fresh insight obtained about the bonding properties between the dopants and the borozenes may also help the design of new metal-doped borophenes or dopant borophene interactions.

Planar B_3 and B_4 clusters have been synthesized as electron-deficient compounds with suitable ligands.[64,65] With the ingenuity of the synthetic chemist, it is conceivable that borozenes or related aromatic boron clusters may also be synthesized or incorporated into bulk compounds.[66] The electron deficiency of boron makes it highly flexible in chemical bonding and in its formation of novel molecules with almost any element in the periodic table. Both metallabenzene analogs of

metallaboron and Mobius aromatic metallaboron clusters have been discovered.[67,68] There is no doubt that new structures and new chemical bonding will continue to be uncovered in the study of size-selected boron clusters and borozene complexes.

AUTHOR INFORMATION

Corresponding Author

Lai-Sheng Wang – *Department of Chemistry, Brown University, Providence, Rhode Island, 02912, United States*; orcid.org/0000-0003-1816-5738; Email: lai-sheng_wang@brown.edu

Notes

The author declares no competing financial interest.

Biography

Lai-Sheng Wang is the Jesse H. and Louisa D. Sharpe Metcalf Professor of Chemistry at Brown University. He received his B.S. degree in chemistry from Wuhan University and his PhD from the University of California at Berkeley. His research group has developed photoelectron spectroscopy techniques to investigate the size-dependent electronic structure and chemical bonding of nanoclusters. More recent work in his lab has focused on the study of the structures and bonding of size-selected boron and boride clusters. His lab has also pioneered electrospray and cryogenic ion trap techniques for photoelectron spectroscopic studies of free multiply-charged anions and complex solution molecules in the gas phase. Recently, they have been focusing on the investigation of polycyclic aromatic hydrocarbon anions and nonvalence excited states in anions using cryogenic photodetachment spectroscopy and resonant photoelectron imaging.

ACKNOWLEDGEMENTS

The author wishes to dedicate this paper to the memory of Prof. Alexander I. Boldyrev, who was a close collaborator for more than two decades on boron clusters and many other topics. I would like to thank my current and former group members who have contributed to this work. I am also indebted to many collaborators, in particular, Prof. Jun Li, Prof. Si-Dian Li, Prof. Ivan Popov and their students for their contributions to the work discussed in this Account. This work was supported by the National Science Foundation under Grant CHE-2403841.

REFERENCES

(1) Li, W. L.; Chen, T. T.; Chen, W. J.; Li, J.; Wang, L. S. Monovalent Lanthanide(I) in Borozene Complexes. *Nature Commun*. **2021**, *12*, 6467.

(2) Tian, W. J.; Chen, W. J.; Yan, M.; Li, R.; Wei, Z. H.; Chen, T. T.; Chen, Q.; Zhai, H. J.; Li, S. D.; Wang, L. S. Transition-Metal-Like Bonding Behaviors of A Boron Atom in A Boron Cluster Boronyl Complex $[(\eta^7\text{-}B_7)\text{-}B\text{-}BO]^-$. *Chem. Sci*. **2021**, *12*, 8157-8164.

(3) Chen, W. J.; Pozdeev, A. S.; Choi, H. W.; Boldyrev, A. I.; Yuan, D. F.; Popov, I. A.; Wang, L. S. Searching for Stable Copper Borozene Complexes in CuB_7^- and CuB_8^-. *Phys. Chem. Chem. Phys*. **2024**, *26*, 12928-12938.

(4) Chen, W. J.; Choi, H. W.; Cavanagh, J.; Yuan, D. F.; Wang, L. S. Electronic Control of the Position of the Pb Atom on the Surface of the B_8 Borozene in the PbB_8 Cluster. *J. Phys. Chem. A* **2024**, *128*, 3564-3570.

(5) Buzea, C.; Yamashita, T. Review of the Superconducting Properties of MgB_2. *Supercond. Sci. Technol*. **2001**, *14*, R115–R146.

(6) Worle, M.; Nesper, R. Infinite, Linear, Unbranched Borynide Chains in LiB_x – Isoelectronic to Polyyne and Polycumulene. *Angew. Chem. Int. Ed*. **2000**, *39*, 2349-2353.

(7) Lipscomb, W. N. The Boranes and Their Relatives. *Science* **1977**, *196*, 1047-1055.

(8) Albert, B.; Hillebrecht, H. Boron: Elementary Challenge for Experimenters and Theoreticians. *Angew. Chem. Int. Ed*. **2009**, *48*, 8640-8668.

(9) Kroto, H. W.; Heath, J. R.; O'Brien, S. C.; Curl, R. F.; Smalley, R. E. C_{60}: Buckminsterfullerene. *Nature* **1985**, *318*, 161-163.

(10) Iijima, S. Helical Microtubules of Graphitic Carbon. *Nature* **1991**, *354*, 56–58.

(11) Novoselov, K. S.; Geim, A. K.; Morozov, S. V.; Jiang, D.; Zhang, Y.; Dubonos, S. V.; Grigorieva, I. V.; Firsov, A. A. Electric Field Effect in Atomically Thin Carbon Films. *Science* **2004**, *306*, 666-669.

(12) Alexandrova, A. N.; Boldyrev, A. I.; Zhai, H. J.; Wang, L. S. All-Boron Aromatic Clusters as Potential New Inorganic Ligands and Building Blocks in Chemistry. *Coord. Chem. Rev*. **2006**, *250*, 2811-2866.

(13) Sergeeva, A. P.; Popov, I. A.; Piazza, Z. A.; Li, W. L.; Romanescu, C.; Wang, L. S.; Boldyrev, A. I. Understanding Boron through Size-Selected Clusters: Structure, Chemical Bonding, and Fluxionality. *Acc. Chem. Res*. **2014**, *47*, 1349-1358.

(14) Wang, L. S. Photoelectron Spectroscopy of Size-Selected Boron Clusters: From Planar Structures to Borophenes and Borospherenes. *Int. Rev. Phys. Chem*. **2016**, *35*, 69-142.

(15) Li, W. L.; Chen, X.; Jian, J.; Chen, T. T.; Li, J.; Wang, L. S. From Planar Boron Clusters to Borophenes and Metalloborophenes. *Nat. Rev. Chem*. **2017**, *1*, 0071.

(16) Jian, T.; Chen, X. N.; Li, S. D.; Boldyrev, A. I.; Li, J.; Wang, L. S. Probing the Structures and Bonding of Size-Selected Boron and Doped-Boron Clusters. *Chem. Soc. Rev*. **2019**, *48*, 3550-3591.

(17) Chen, T. T.; Cheung, L. F.; Wang, L. S. Probing the Nature of the Transition-Metal Boron Bonds and Novel Aromaticity in Small Metal-Doped Boron Clusters Using Photoelectron spectroscopy. *Annu. Rev. Phys. Chem*. **2022**, *73*, 233-253.

(18) Zhai, H. J.; Kiran, B.; Li, J.; Wang, L. S. Hydrocarbon Analogs of Boron Clusters: Planarity, Aromaticity, and Antiaromaticity. *Nature Mater.* **2003**, *2*, 827-833.

(19) Sergeeva, A. P.; Zubarev, D. Y.; Zhai, H. J.; Boldyrev, A. I.; Wang, L. S. A Photoelectron Spectroscopic and Theoretical Study of B_{16}^- and B_{16}^{2-}: An All-Boron Naphthalene. *J. Am. Chem. Soc*. **2008**, *130*, 7244-7246.

(20) Sergeeva, A. P.; Piazza, Z. A.; Romanescu, C.; Li, W. L.; Boldyrev, A. I.; Wang, L. S. B_{22}^- and B_{23}^-: All-Boron Analogues of Anthracene and Phenanthrene. *J. Am. Chem. Soc.* **2012**, *134*, 18065-18073.

(21) Piazza, Z. A.; Hu, H. S.; Li, W. L.; Zhao, Y. F.; Li, J.; Wang, L. S. Planar Hexagonal B_{36} as a Potential Basis for Extended Single-Atom Layer Boron Sheets. *Nature Commun*. **2014**, *5*, 3113.

(22) Mannix, A. J.; Zhou, X. F.; Kiraly, B.; Wood, J. D.; Alducin, D.; Myers, B. D.; Liu, X.; Fisher, B. L.; Santiago, U.; Guest, J. R.; Yacaman, M. J.; Ponce, A.; Oganov, A. R.; Hersam, M. C.; Guisinger, N. P. Synthesis of Borophenes: Anisotropic, Two-Dimensional Boron Polymorphs. *Science* **2015**, *350*, 1513-1516

(23) Feng, B.; Zhang, J.; Zhong, Q.; Li, W.; Li, S.; Li, H.; Cheng, P.; Meng, S.; Chen, L.; Wu, K. Experimental Realization of Two-Dimensional Boron Sheets. *Nat. Chem.* **2016**, *8*, 563-568.

(24) Kaneti, Y. V.; Benu, D. P.; Xu, X.; Yuliarto, B.; Yamauchi, Y.; Golberg, D. Borophene: Two-dimensional Boron Monolayer: Synthesis, Properties, and Potential Applications. *Chem. Rev.* **2022**, *122*, 1000−1051.

(25) Zhai, H. J.; Zhao, Y. F.; Li, W. L.; Chen, Q.; Bai, H.; Hu, H. S.; Piazza, Z. A.; Tian, W. J.; Lu, H. G.; Wu, Y. B.; Mu, Y. W.; Wei, G. F.; Liu, Z. P.; Li, J.; Li, S. D.; Wang, L. S. Observation of an All-Boron Fullerene. *Nature*

Chem. **2014**, *6*, 727-731.

(26) Zhai, H. J.; Wang, L. S.; Alexandrova, A. N.; Boldyrev, A. I. On the Electronic Structure and Chemical Bonding of B_5^- and B_5 by Photoelectron Spectroscopy and *Ab Initio* Calculations. *J. Chem. Phys*. **2002**, *117*, 7917-7924.

(27) Alexandrova, A. N.; Boldyrev, A. I.; Zhai, H. J.; Wang, L. S.; Steiner, E.; Fowler, P. W. Structure and Bonding in B_6^- and B_6: Planarity and Antiaromaticity. *J. Phys. Chem*. A **2003**, *107*, 1359-1369.

(28) Zhai, H. J.; Alexandrova, A. N.; Birch, K. A.; Boldyrev, A. I.; Wang, L. S. Hepta- and Octacoordinated Boron in Molecular Wheels of Eight- and Nine-Atom Boron Clusters: Observation and Confirmation. *Angew. Chem. Int. Ed*. **2003**, *42*, 6004-6008.

(29) Alexandrova, A. N.; Zhai, H. J.; Wang, L. S.; Boldyrev, A. I. Molecular Wheel B_8^{2-} as a New Inorganic Ligand. Photoelectron Spectroscopy and *Ab Initio* Characterization of LiB_8^-. *Inorg. Chem*. **2004**, *43*, 3553-3554.

(30) Alexandrova, A. N.; Boldyrev, A. I.; Zhai, H. J.; Wang, L. S. Electronic Structure, Isomerism, and Chemical Bonding in B_7^- and B_7. *J. Phys. Chem*. A **2004**, *108*, 3509-3517.

(31) Romanescu, C.; Galeev, T. R.; Li, W. L.; Boldyrev, A. I.; Wang, L. S. Transition-Metal-Centered Monocyclic Boron Wheel Clusters (M©B_n): A New Class of Aromatic Borometallic Compounds. *Acc. Chem. Res*. **2013**, *46*, 350-358.

(32) Barroso, J.; Pan, S.; Merino, G. Structural Transformations in Boron Clusters Induced by Metal Doping. *Chem. Soc. Rev*. **2022**, *51*, 1098–1123.

(33) Chen, B.; He, K.; Dai, W.; Gutsev, G. L.; Lu, C. Geometric and Electronic Diversity of Metal Doped Boron Clusters. *J. Phys.: Condens. Matter* **2023**, *35*, 183002.

(34) Pan, L. L.; Li, J.; Wang, L. S. Low-Lying Isomers of the B_9^- Boron Cluster: the Planar Molecular Wheel versus Three-Dimensional Structures. *J. Chem. Phys*. **2008**, *129*, 024302.

(35) Banerjee, S.; Periyasamyb, G.; Pati, S. K. Density Functional Theoretical Investigation on Structure, Optical Response and Hydrogen Adsorption Properties of B_9/Metal–B_9 Clusters. *Phys. Chem. Chem. Phys*. **2013**, *15*, 8303-8310.

(36) Galeev, T. R.; Romanescu, C.; Li, W. L.; Wang, L. S.; Boldyrev, A. I. Valence Isoelectronic Substitution in the B_8^- and B_9^- Molecular Wheels by an Al Dopant Atom: Umbrella-like Structures of AlB_7^- and AlB_8^-. *J. Chem. Phys*. **2011**, *135*, 104301.

(37) Chen, T. T.; Li, W. L.; Jian, T.; Chen, X.; Li, J.; Wang, L. S. PrB_7^-: A Praseodymium-Doped Boron Cluster with a Pr^{II} Center Coordinated by a Doubly Aromatic Planar η^7-B_7^{3-} Ligand. *Angew. Chem. Int. Ed*. **2017**, *56*, 6916-6920.

(38) Zubarev D. Y.; Boldyrev, A. I. Developing Paradigms of Chemical Bonding: Adaptive Natural Density Partitioning. *Phys. Chem. Chem. Phys*. **2008**, *10*, 5207–5217.

(39) Jia, J.; Ma, L.; Wang, J. F.; Wu, H. S. Structures and Stabilities of ScB_n (n = 1–12) Clusters: An Ab Initio Investigation. *J. Mol. Model*. **2013**, *19*, 3255–3261.

(40) Chen, W. J.; Kulichenko, M.; Choi, H. W.; Cavanagh, J.; Yuan, D. F.; Boldyrev, A. I.; Wang, L. S. Photoelectron Spectroscopy of Size-Selected Bismuth-Boron Clusters: BiB_n^- (n = 6–8). *J. Phys. Chem. A* **2021**, *125*, 6751-6760.

(41) Saha, P.; Rahane, A. B.; Kumar, V.; Sukumar, N. Analysis of the Electron Density Features of Small Boron Clusters and the Effects of Doping with C, P, Al, Si, and Zn: Magic B_7P and B_8Si Clusters. *Phys. Scr*. **2016**, *91*, 053005.

(42) Feng, X.; Shi, D.; Jia, J.; Wang, C. Structural Evolution and Electronic Properties of Germanium-Doped Boron Clusters and Their Anions: $GeB_n^{0/-}$ (n = 6–20). *J. Nanopart. Res*. **2022**, *24*, 124.

(43) Reber, A. C.; Khanna, S. N. Electronic Structure, Stability, and Oxidation of Boron-Magnesium Clusters and Cluster Solids. *J. Chem. Phys*. **2015**, *142*, 054304.

(44) Yu, R.; Barroso, J.; Wang, M.-h.; Liang, W.-y.; Chen, C.; Zarate, X.; Orozco-Ic, M.; Cui, Z.-h.; Merino, G. Structure and Bonding of Molecular Stirrers with Formula $B_7M_2^-$ and B_8M_2 (M = Zn, Cd, Hg). *Phys. Chem. Chem. Phys*. **2020**, *22*, 12312-12320.

(45) Wang, W.; Wang, J.; Gong, C.; Mu, C.; Zhang, D.; Zhang, X. Designer Mg-Mg and Zn-Zn Single Bonds Facilitated by Double Aromaticity in the $M_2B_7^-$ (M = Mg, Zn) Clusters. *Chin. J. Chem. Phys*. **2020**, *33*, 578–582.

(46) Resa, I.; Carmona, E.; Gutierrez-Puebla, E.; Monge, A. Decamethyldizincocene, a Stable Compound of Zn(I) with a Zn–Zn Bond. *Science* **2004**, *305*, 1136-1138.

(47) Green, S. P.; Jones, C.; Stasch, A. Stable Magnesium(I) Compounds with Mg-Mg Bonds. *Science* **2007**, *318*, 1754-1757.

(48) Boronski, J. T.; Crumpton, A. E.; Wales, L. L.; Aldridge, S. Diberyllocene, a Stable Compound of Be(I) with a Be–Be Bond. *Science* **2023**, *380*, 1147-1149.

(49) Wang, Y. J.; Feng, L. Y.; Zhai, H. J. Sandwich-Type $Na_6B_7^-$ and $Na_8B_7^+$ Clusters: Charge-Transfer Complexes, Four-Fold π/σ Aromaticity, and Dynamic Fluxionality. *Phys. Chem. Chem. Phys*. **2019**, *21*, 18338-18345.

(50) Zhai, H. J.; Chen, Q.; Bai, H.; Li, S. D.; Wang , L. S. Boronyl Chemistry: The BO Group as a New Ligand in Gas-Phase Clusters and Synthetic Compounds. *Acc. Chem. Res.* **2014**, *47*, 2435-2445.

(51) Legare, M.-A.; Pranckevicius, C.; Braunschweig, H. Metallomimetic Chemistry of Boron. *Chem. Rev*. **2019**, *119*, 8231−8261.

(52) Li, W. L.; Burkhardt, J. AnB_8^-: Borozene Complexes with Monovalent Actinide. *Phys. Chem. Chem. Phys*. **2024**, *26*, 16091-16095.

(53) Chen, C.; Lv, H.; Zhang, P.; Zhuo, Z.; Wang, Y.; Ma, C.; Li, W.; Wang, X.; Feng, B.; Cheng, P.; Wu, X.; Wu, K.; Chen, L. Synthesis of Bilayer Borophene. *Nat. Chem*. **2022**, *14*, 25-31.

(54) Pozdeev, A. S.; Chen, W. J.; Kulichenko, M.; Choi, H. W.; Boldyrev, A. I.; Wang, L. S. On the Structures and Bonding of Copper Boride Nanoclusters, $Cu_2B_x^-$ (*x* = 5–7). *Solid State Sci.* **2023**, *142*, 107248.

(55) Pozdeev, A. S.; Chen, W. J.; Choi, H. W.; Kulichenko, M.; Yuan, D. F.; Boldyrev, A. I.; Wang, L. S. A Photoelectron Spectroscopy and Theoretical Study of Di-Copper Boron Clusters: $Cu_2B_3^-$ and $Cu_2B_4^-$. *J. Phys. Chem. A* **2023**, *127*, 4888-4896.

(56) Pyykko, P. Relativistic Effects in Structural Chemistry. *Chem. Rev*. **1988**, *88*, 563-594.

(57) Wang, L. S. Covalent Gold. *Phys. Chem. Chem. Phys*. **2010**, *12*, 8694-8705.

(58) Chen, W. J.; Zhang, Y. Y.; Li, W. L.; Choi, H. W.; Li, J.; Wang, L. S. AuB_8^-: An Au-Borozene Complex. *Chem. Comm*. **2022**, *58*, 3134-3137.

(59) Kulichenko, M.; Chen, W. J.; Choi, H. W.; Yuan, D. F.; Boldyrev, A. I.; Wang, L. S. Probing Copper-Boron Interactions in the $Cu_2B_8^-$ Bimetallic Cluster. *J. Vac. Sci Technol. A* **2022**, *40*, 042201.

(60) Wang, Y. J.; Feng, L. Y.; Guo, J. C.; Zhai, H. J. Dynamic Mg_2B_8 Cluster: A Nanoscale Compass, *Chem. Asian J*. **2017**, *12*, 2899-2903.

(61) Liao, Y.; Cruz, C. L.; Schleyer, P. v. R.; Chen. Z. Many M©B_n Boron Wheels Are Local, But Not Global Minima. *Phys. Chem. Chem. Phys*. **2012**, *14*, 14898–14904.

(62) Mai, D. T. T.; Duong, L. V.; Tai, T. B.; Nguyen, M. T. Electronic Structure and Thermochemical Parameters of the Silicon-Doped Boron Clusters B_nSi, with *n* = 8−14, and Their Anions. *J. Phys. Chem. A* **2016**, *120*, 3623-3633.

(63) Averkiev, B. B.; Wang, L. M.; Huang, W.; Wang, L. S.; Boldyrev, A. I. Experimental and Theoretical Investigations of CB_8^-: Towards Rational Design of Hypercoordinated Planar Chemical Species. *Phys. Chem. Chem. Phys*. **2009**, *11*, 9840-9849.

(64) Himmel, H.-J. Electron-Deficient Triborane and Tetraborane Ring Compounds: Synthesis, Structure, and Bonding. *Angew. Chem. Int. Ed*. **2019**, *58*, 11600–11617.

(65) Kar, S.; Bairagi, S.; Kar, K.; Roisnel, T.; Dorcet, V.; Ghosh, S. Metal Coordinated Tri- and Tetraborane Analogues. *Eur. J. Inorg. Chem*. **2021**, 4443–4451.

(66) Scheifers, J. P.; Zhang, Y.; Fokwa, B. P. T. Boron: Enabling Exciting Metal-Rich Structures and Magnetic Properties. *Acc. Chem. Res*. **2017**, *50*, 2317−2325.

(67) Cheung, L. F.; Czekner, J.; Kocheril, G. S.; Wang, L. S. ReB_6^-: A Metallaboron Analog of Metallabenzenes. *J. Am. Chem. Soc*. **2019**, *141*, 17854-17860.

(68) Cheung, L. F.; Kocheril, G. S.; Czekner, J.; Wang, L. S. Observation of Möbius Aromatic Planar Metallaborocycles. *J. Am. Chem. Soc*. **2020**, *141*, 3356-3360.